Pullulan mediated zinc oxide microparticles: Effect of synthesis temperature

E D Mohamed Isa[1], N W Che Jusoh[2,3], R Hazan[4] and K Shameli[1,*]

[1]Department of Environmental and Green Technology, Malaysia-Japan International Institute of Technology, Universiti Teknology Malaysia, Jalan Sultan Yahya Petra, 54100 Kuala Lumpur Malaysia
[2]Department of Chemical Process Engineering, Malaysia-Japan International Institute of Technology, Universiti Teknology Malaysia, Jalan Sultan Yahya Petra, 54100 Kuala Lumpur Malaysia
[3]Advanced Materials Research Group, Center of Hydrogen Energy, Universiti Teknologi Malaysia, 54100, Kuala Lumpur, Malaysia.
[4]Malaysian Nuclear Agency, Bangi, 43000 Kajang, Selangor, Malaysia

*kamyarshameli@gmail.com

Abstract. Zinc oxide (ZnO) has been gaining a lot of attention compared to the other semiconductor metal oxide. This is due to their favourable properties such as chemical stability, high electrochemical coupling coefficient, broad range of absorption radiation and high photostability. It also has wide band gap energy (3.37 eV), large exciton-binding energy (60 meV) and high thermal and mechanical stability at room temperature. Besides these desirable properties, the synthesis of ZnO has been widely studied as it is easy to synthesized and its properties such as band gap, shape and size can be controlled through synthesis parameters and methods. In this study, zinc oxide microparticles (ZnO-MCs) is produced with pullulan as mediator via precipitation method. The effect of synthesis temperature on the properties of synthesized ZnO-MCs were also studied. Based on the result obtained, all synthesized ZnO-MCs exhibited hexagonal wurtzite structure. As the synthesis temperature increases, the particles morphology changes from large spherical shape to flower-like morphology. Furthermore, the particle size also decreases with increasing temperature. This result is supported by surface area and pore analysis where the surface area ranging from 6.22 to 22.78 m^2 g^{-1} was obtained as the synthesis temperature increases. All these results indicate that synthesis method and parameters will affect the properties of synthesized ZnO-MCs.

1. Introduction

Zinc oxide (ZnO) is an important II-IV compound semiconductor and it has been widely studied within the context of nanoscience and nanotechnology [1]. The interest on ZnO is due to their unique physical and chemical properties such as chemical stability, high electrochemical coupling coefficient, broad range of absorption radiation and high photostability. Furthermore, it also has wide band gap energy (3.37 eV), large exciton-binding energy (60 meV) and high thermal and mechanical stability at room temperature. All these properties can be tuned according to desire by controlling the synthesis process and parameters. [2].

In these recent years, green synthesis has been the main focus in synthesized ZnO. Green synthesis is defined as synthesis process that utilized natural products such as plant extracts, microorganisms and

biopolymers to produce the materials. Biopolymers such as carbohydrate has been used as one of the green materials to produce ZnO. Taghavi et al reported the production of ZnO nanoparticles using arabic gum via sol-gel method [3]. Soraya et al also reported the usage of Tragacanth gum as reducing and stabilizing agent in production of urchin-like ZnO nanorods array. To produce urchin-like ZnO, they utilized combination method of precipitation and ultrasound method [4].

Pullulan is a biopolymer that is produced from starch by growing yeast like fungus *Aureobasidium pullulans*. The advantage of pullulan is it is water soluble. It is made out of maltotriose which consist of three glucose units linked by an α-(1,4) glycosidic bond and the maltotriose units are linked by an α-(1,6) glycosidic bond. Pullulan is non-toxic, non-mutagenic, odourless, biocompatible and biodegradable [5]. It also has wide range of commercial and industrial applications across various fields. Previous study shows that pullulan has been used as stabilizer to produce gold nanoparticles [6]. In a much recent works, pullulan has been used to produce ceria nanoparticles [7]. Currently, there is no works that reported on the usage of pullulan in production of ZnO.

In this study, pullulan is used as stabilizer to produce ZnO microparticles (ZnO-MCs) via precipitation method. The effect of synthesis temperature on the properties of ZnO-MCs were studied.

2. Materials and methodology

2.1 Materials

Pullulan powder (99%) was purchased from China. Chemicals of analytical grade, zinc nitrate hexahydrate ($Zn(NO_3)_2 \cdot 6H_2O$, 98 %) and ammonia solution (30 % NH_3 in water) were purchased from R & M Chemicals, Malaysia.

2.2 Synthesis of ZnO microparticles by precipitation method

4 sets of experiments for the ZnO-MCs were performed by varying the synthesis temperature (room temperature, 40 °C, 60 °C and 80 °C). In a typical run, 5 g of pullulan was dissolved in 150 mL water. 2.97 g of $Zn(NO_3)_2 \cdot 6H_2O$ was added to the solution and the mixture was stirred at 60 °C for 5 minutes. Then 3 mL of ammonia solution was added to the mixture and stirred for another 30 minutes. The resulting precipitate was centrifuged, washed with water and dried overnight in an over at 50 °C. Then, the obtained powders were calcined at 500 °C for 1 hour. The samples were named RTZ, 4TZ, 6TZ and 8TZ according to synthesis temperature of room temperature, 40 °C, 60 °C and 80 °C respectively.

2.3 Characterization

The X-ray diffraction (XRD) analysis of synthesized ZnO-MCs were carried out by using the PANalytical X'pert Pro MPD diffractometer with Cu K_α radiation ($\lambda = 1.5406$) in the 2θ range from 20° to 80°. The surface morphology of ZnO-MCs were analysed using field emission electron microscope (FESEM) model Carl Zeiss GeminiSEM 500. The surface area and pore analysis was conducted using Quantachrome Instrument Novatouch. The samples were degas at 150 °C for 4 hours before analysis. Fourier Transform Infrared (FTIR) spectra were recorded over the range of 400-4000 cm^{-1} by using Shimadzu IRTracer-100 with potassium bromide (KBr) pellet method. Diffuse reflectance spectra (DRS) were collected on Shimadzu UV-2600 spectrophotometer with an integrating sphere accessory.

3. Results and discussion

The XRD patterns of synthesized ZnO-MCs at different synthesis temperature are shown in figure 1. The XRD spectra for all synthesizde ZnO-MCs were very similar, all exhibiting characteristic diffraction peaks at 2θ = 31.8°, 34.4°, 36.3°, 47.6°, 56.6° and 62.8° corresponding well to the (100), (002), (101), (102), (110) and (103) crystal planes of hexagonal wurtzite ZnO (JCPDS No. 36-1451) [8, 9]. Besides that, no characteristic peaks for impurities were observed and this indicate that the prepared ZnO-MCs samples have high purity. Furthermore, strong and sharp diffraction peaks indicate that the materials have high crystallinity. It is observed that as the synthesis temperature increases, the peak intensities decrease. This indicates that the particle size decreases with increasing synthesis temperature

as reported by Olieveira et al [10]. The crystallite size of ZnO-MCs can be calculated from the full width at half maximum (FWHM) of XRD patterns using Scherer formula as shown in equation (1):

$$D = \frac{0.9\lambda}{\beta cos\theta} \quad (1)$$

Where λ is the wavelength of the Cu Kα radiation, β is the FWHM of the peak and θ is the Bragg angle [3, 11]. Using the formula, the average size of ZnO-MCs were 22.76, 24.39, 22.76 and 18.98 nm for RTZ, 4TZ, 6TZ and 8TZ respectively.

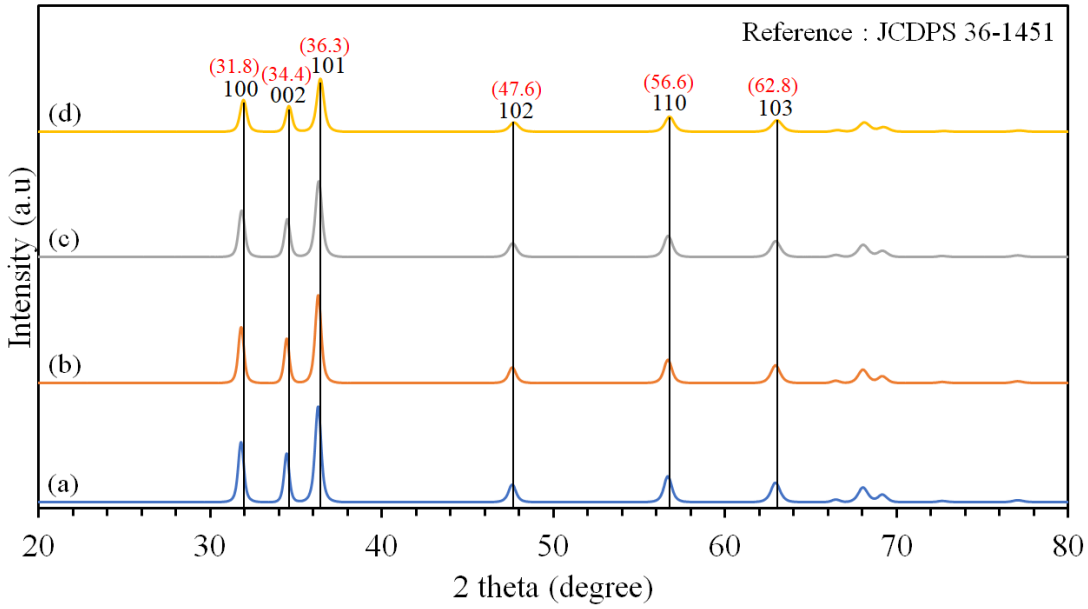

Figure 1. The XRD of synthesized ZnO-MCs. (a) RTZ, (b) 4TZ, (c) 6TZ and (d) 8TZ.

The particles morphology was then further studied using FESEM and Figure 2 shows that all the FESEM images of synthesized ZnO-MCs. RTZ exhibited various morphologies which consist of mixture of spherical and large flower-like structures. As the reaction temperature increases, it can be seen that the particles start to more define flower-like morphology. Besides that, as the temperature increases, the overall size of ZnO-MCs decreases. At higher synthesis temperature, nucleation process is conducive and this leads to lower particles growth rate. This will then lead to smaller particles size. This observation is similar to previous reports [12, 13]. Another unique property of synthesized ZnO-MCs that can be observed through FESEM is the presence of pores within the particles.

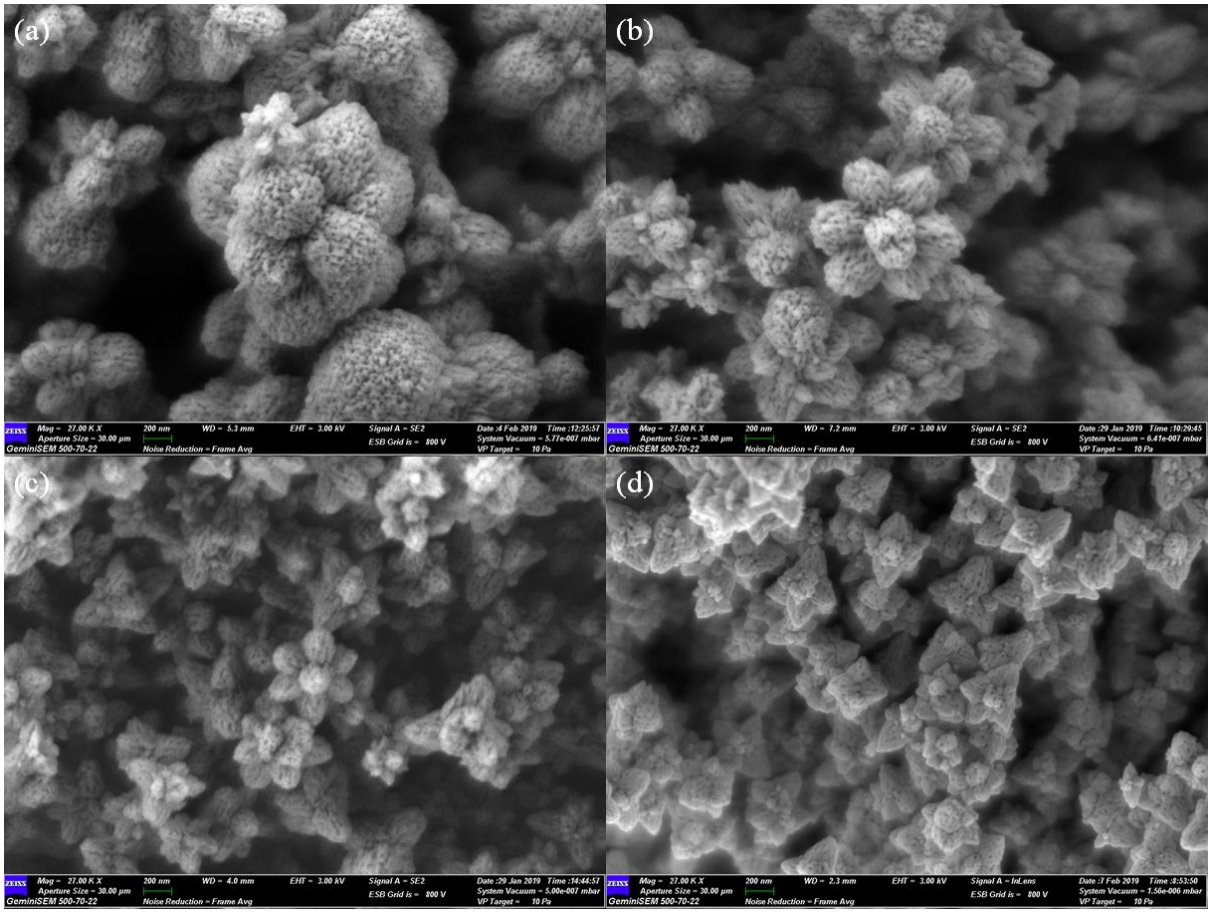

Figure 2. FESEM images of ZnO-MCs. (a) RTZ, (b) 4TZ, (c) 6TZ and (d) 8TZ.

Based on FESEM analysis, it was found that all synthesized ZnO-MCs exhibited some porosity. Therefore, to confirm the presence of pores within the ZnO-MCs, the compounds were analysed through surface area and pore analysis. The nitrogen adsorption-desorption isotherm of all synthesized ZnO-MCs and its respective pore size distribution are shown in Figure 3. It can be seen that all ZnO-MCs exhibit type IV isotherm which indicate the presence of mesopore [11]. This result is in agreement with the FESEM images obtained where there was porosity observed in all synthesize ZnO-MCs. Besides that, from the isotherm, it is also observe that there were hysteresis loops at relatively high pressure and this might be due to presence of large pores of interparticle spaces [11, 14]. From the nitrogen sorption analysis, the BET surface areas were obtained for RTZ, 4TZ, 6TZ and 8TZ where surface area of 20.93, 19.05, 22.78 and 22.60 $m^2 g^{-1}$ were observed respectively. The general trend of increasing BET surface area with increasing synthesis temperature was observed. The is due to the decrease of particles size as smaller particles size have higher surface area value [15].

(a)

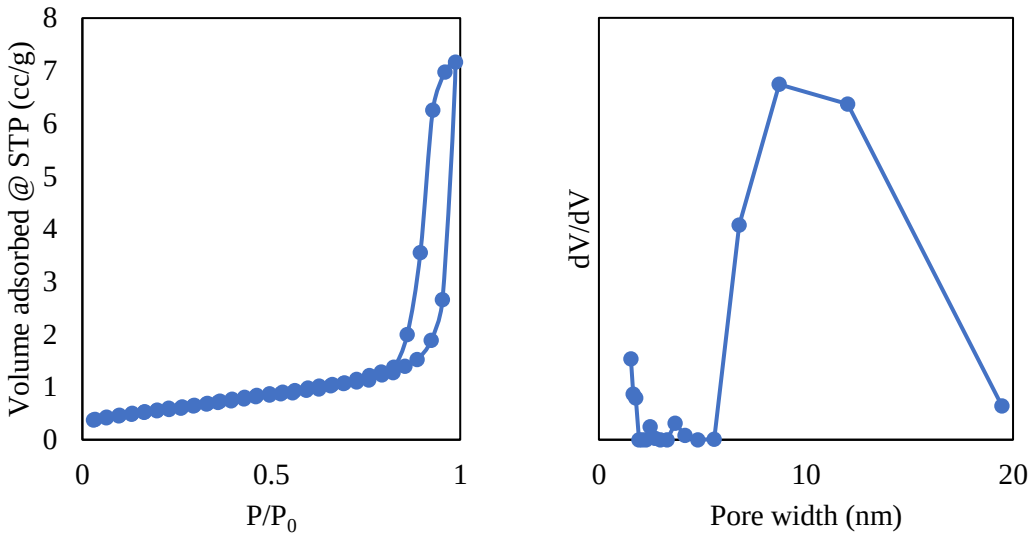
Volume adsorbed @ STP (cc/g)
0
1
2
3
4
5
6
7
8
0
0.5
1
P/P0
dV/dV
0
10
20
Pore width (nm)

(b)

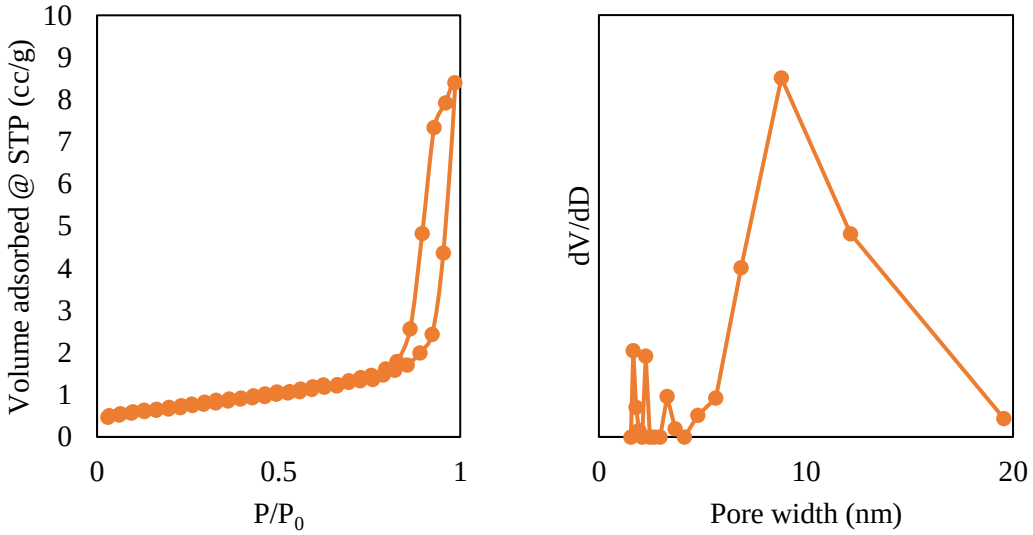
Volume adsorbed @ STP (cc/g)
0
1
2
3
4
5
6
7
8
9
10
0
0.5
1
P/P0
dV/dD
0
10
20
Pore width (nm)

(c)

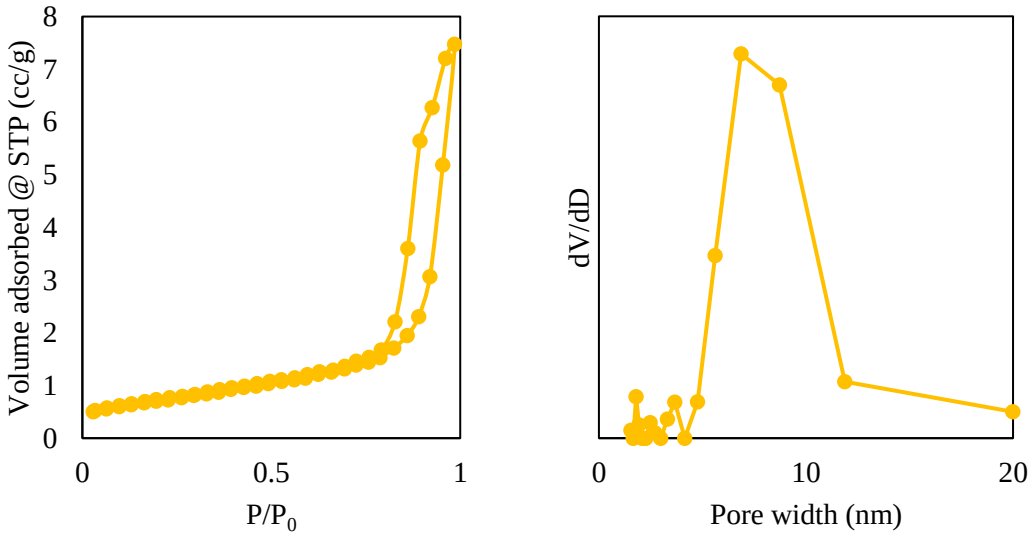
Volume adsorbed @ STP (cc/g)
0
1
2
3
4
5
6
7
8
0
0.5
1
P/P0
dV/dD
0
10
20
Pore width (nm)

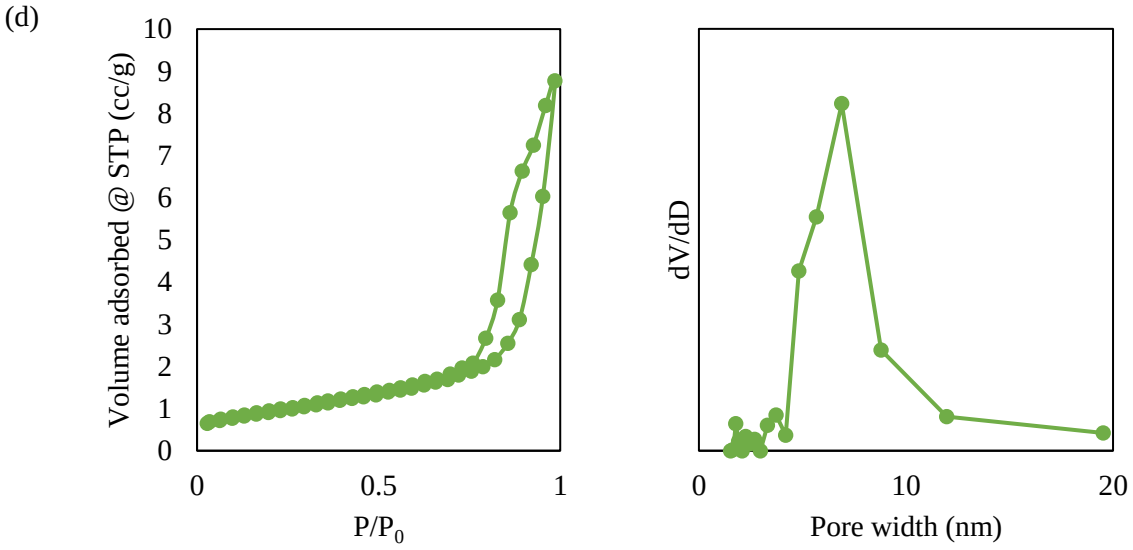

Figure 3. Nitrogen adsorption-desorption isotherm and pore distribution plot of ZnO-MCs. (a) RTZ, (b) 4TZ, (c) 6TZ and (d) 8TZ

The formation of ZnO-MCs was further investigated using FTIR analysis. Figure 4 shows the FTIR spectra of pullulan, synthesized ZnO-MCs before calcination and ZnO-MCs after calcination. In pullulan spectrum, there were two strong absorption bands at 3300 and 2916 cm^{-1} and this is due to OH stretching vibration and sp^3 C-H bond respectively. Single band at 1631 cm^{-1} was assigned to stretching vibration of O-C-O in pullulan. Other features bands of pullulan were also observed around 1358 and 1147 cm^{-1} which correspond to C-O-H bend and C-O-C stretch respectively. Besides that, the typical pullulan band, α-configuration of α-D-glucopyranose units was also observed around 840 cm^{-1}. Furthermore, two bands representing the linkages of pullulan were also found around 925 and 752 cm^{-1}. All the bands observed in the pullulan spectrum are similar to the previously reported works [16, 17].

Through comparison of pullulan's FTIR spectrum with ZnO-MCs before calcination FTIR spectrum, characteristic bands of pullulan could be observed in sample before calcination. It was found that the band at around 840 and 925 cm^{-1} which represent pullulan bands present although at low intensity. This might be due to low presence of pullulan as the sample was washed with water before the analysis. These bands completely disappear in calcined ZnO-MCs spectrum which indicate that the pullulan has been completely removed through calcination. Presence of new peak around 400 cm^{-1} for both before calcination and calcined ZnO-MCs spectra was assigned to Zn-O.

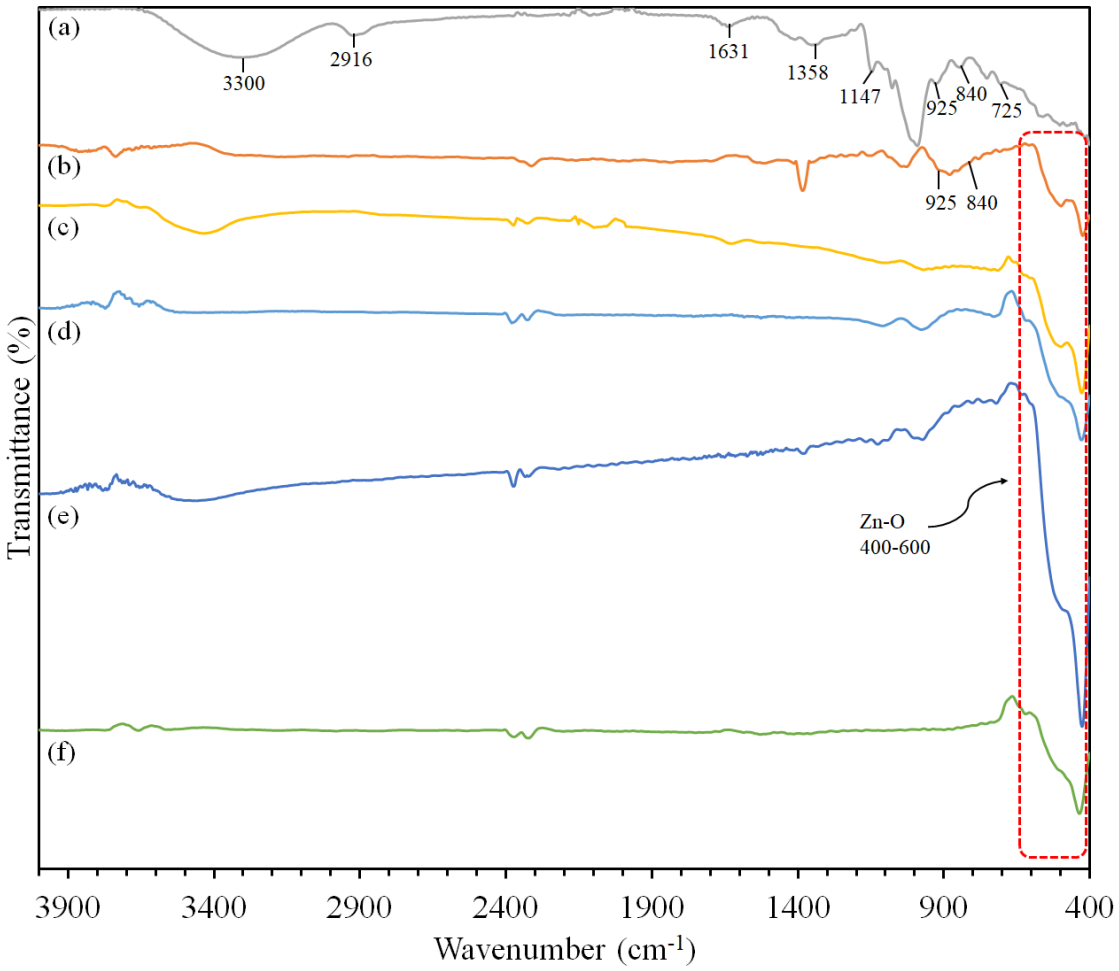

Figure 4. FTIR spectra of (a) pullulan, (b) ZnO-MCs before calcination, (c) RTZ, (d) 4TZ, (e) 6TZ and (f) 8TZ.

The optical properties of synthesized ZnO-MCs were determined through UV-Vis diffuse reflectance. Figure 5 shows the UV-Vis diffuse reflectance spectra of the ZnO-MCs generated at different synthesis temperatures. It can be seen that the reflectance increases at wavelength above 370 nm and this is can be assigned to the direct band gap of ZnO. This is due to electron transitions from the valence band to the conduction band [18]. As ZnO is a direct band gap semiconductor, its band gap energy (E_g) can be determined from equation (2):

$$(\alpha hv)^2 = A(hv - E_g) \quad (2)$$

where α, h, v, E_g and A are the absorption coefficient, Planck's constant light frequency, band hap energy and a constant respectively. The E_g values of the ZnO-MCs samples can be obtained by plotting a graph of $(\alpha hv)^2$ against hv [9]. Through extrapolating the linear portion of the curves to zero, it was found that the E_g values of all the synthesized ZnO were ~3.2 eV.

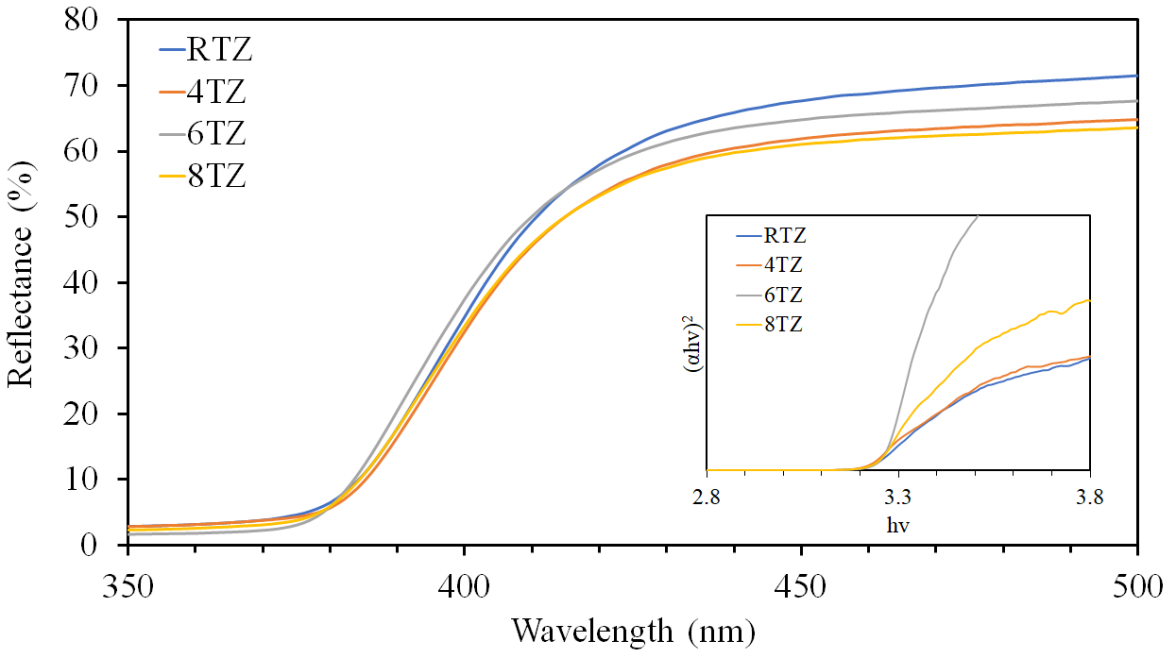

Figure 5. UV-VIS diffuse reflectance spectra of all synthesized ZnO-MCs at different synthesis temperatures. Inset: The corresponding plots of $(\alpha hv)^2$ versus energy (hv) for the band gap energy of ZnO-MCs.

4. Conclusion

In this study, ZnO-MCs were successfully synthesized with pullulan as mediator. The effect of synthesis temperature on the properties of ZnO-MCs were determined. All synthesized ZnO-MCs exhibited hexagonal wurtzite structure. Based on FESEM analysis, it was observed that the particles evolved from large spherical microparticles to flower-like microparticles. Furthermore, as the synthesis temperature increases, the ZnO-MCs particle size decreases which also lead to increase of surface area value. The optical properties of synthesized ZnO-MCs were determined through UV-VIS diffuse reflectance and all the synthesized ZnO-MCs exhibited similar band gap value of ~3.2 eV.

Acknowledgement

The author wish to acknowledged funding by the Malaysian Ministry of Higher Education under the Tier 1 grant (Grant no. #20H33 and #20H55) and express gratitude to the Research Management Centre (RMC) of UTM and Malaysia-Japan International Institute of Technology (MJIIT) for providing an excellent research environment and facilities.

References

[1] Ma Q, Wang Y, Kong J, Jia H and Wang Z 2015 Controllable synthesis of hierarchical flower-like ZnO nanostructures assembled by nanosheets and its optical properties *Superlattices and Microstructures* **84** 1-12

[2] Yıldırım Ö A and Durucan C 2012 Effect of precipitation temperature and organic additives on size and morphology of ZnO nanoparticles *Journal of Materials Research* **27** 1452-61

[3] Taghavi Fardood S, Ramazani A, Moradi S and Azimzadeh Asiabi P 2017 Green synthesis of zinc oxide nanoparticles using arabic gum and photocatalytic degradation of direct blue 129 dye under visible light *Journal of Materials Science: Materials in Electronics* **28** 13596-601

[4] Ghayempour S, Montazer M and Mahmoudi Rad M 2016 Tragacanth gum biopolymer as reducing and stabilizing agent in biosonosynthesis of urchin-like ZnO nanorod arrays: A low

cytotoxic photocatalyst with antibacterial and antifungal properties *Carbohydr Polym* **136** 232-41
[5] Ganeshkumar M, Ponrasu T, Raja M D, Subamekala M K and Suguna L 2014 Green synthesis of pullulan stabilized gold nanoparticles for cancer targeted drug delivery *Spectrochim Acta A Mol Biomol Spectrosc* **130** 64-71
[6] Laksee S, Puthong S, Teerawatananond T, Palaga T and Muangsin N 2017 Highly efficient and facile fabrication of monodispersed Au nanoparticles using pullulan and their application as anticancer drug carriers *Carbohydr Polym* **173** 178-91
[7] Khorrami M B, Sadeghnia H R, Pasdar A, Ghayour-Mobarhan M, Riahi-Zanjani B and Darroudi M 2018 Role of Pullulan in preparation of ceria nanoparticles and investigation of their biological activities *Journal of Molecular Structure* **1157** 127-31
[8] Wang S, Kuang P, Cheng B, Yu J and Jiang C 2018 ZnO hierarchical microsphere for enhanced photocatalytic activity *Journal of Alloys and Compounds* **741** 622-32
[9] He L, Tong Z, Wang Z, Chen M, Huang N and Zhang W 2018 Effects of calcination temperature and heating rate on the photocatalytic properties of ZnO prepared by pyrolysis *J Colloid Interface Sci* **509** 448-56
[10] Oliveira A P A, Hochepied J-F, Grillon F and Berger M-H 2003 Controlled Precipitation of Zinc Oxide Particles at Room Temperature *Chemistry of Materials* **15** 3202-7
[11] Zhang G, Shen X and Yang Y 2011 Facile Synthesis of Monodisperse Porous ZnO Spheres by a Soluble Starch-Assisted Method and Their Photocatalytic Activity *The Journal of Physical Chemistry C* **115** 7145-52
[12] Mohammed Fayaz A, Balaji K, Kalaichelvan P T and Venkatesan R 2009 Fungal based synthesis of silver nanoparticles--an effect of temperature on the size of particles *Colloids Surf B Biointerfaces* **74** 123-6
[13] Khalil M M H, Ismail E H, El-Baghdady K Z and Mohamed D 2014 Green synthesis of silver nanoparticles using olive leaf extract and its antibacterial activity *Arabian Journal of Chemistry* **7** 1131-9
[14] Li X, Shi B, Wang Y, Li M, Liu Y, Gao L and Mao L 2015 Preparation of monodispersed mesoporous silica particles and their applications in adsorption of Au 3+ and Hg 2+ after mercapto-functionalized treatment *Microporous and Mesoporous Materials* **214** 15-22
[15] Yu M, Zhou L, Zhang J, Yuan P, Thorn P, Gu W and Yu C 2012 A simple approach to prepare monodisperse mesoporous silica nanospheres with adjustable sizes *J Colloid Interface Sci* **376** 67-75
[16] Saber-Samandari S, Gulcan H O, Saber-Samandari S and Gazi M 2014 Efficient Removal of Anionic and Cationic Dyes from an Aqueous Solution Using Pullulan-graft-Polyacrylamide Porous Hydrogel *Water Air and Soil Pollution* **225**
[17] Shingel K I 2002 Determination of structural peculiarities of dexran, pullulan and γ-irradiated pullulan by Fourier-transform IR spectroscopy *Carbohydrate Research* **337** 1445-51
[18] Khorsand Zak A, Abd. Majid W H, Mahmoudian M R, Darroudi M and Yousefi R 2013 Starch-stabilized synthesis of ZnO nanopowders at low temperature and optical properties study *Advanced Powder Technology* **24** 618-24